

Nuclear polarization effects in Coulomb excitation studies

J.N. Orce

Department of Physics, University of the Western Cape, P/B X17, Bellville, ZA-7535 South Africa

Abstract

New polarization potentials have been determined based on: 1) the latest photo-neutron cross section evaluation and a missing factor of two in previous work, and 2) the mass dependency of the symmetry energy, $a_{sym}(A)$. The magnitude of the first one is 54% stronger than the currently accepted polarization potential. The second one opens up the possibility for a parameter-free polarization potential. Both polarization potentials are essentially the same for heavy nuclei. The polarization effect on quadrupole collectivity is more substantial than previously assumed for light nuclei. Particular cases are discussed where long-standing discrepancies between high-precision Coulomb-excitation and lifetime measurements still remain. A solution to the long-standing discrepancy between $B(E2; 0_1^+ \rightarrow 2_1^+)$ values determined in ^{18}O by several Coulomb-excitation studies and a high-precision lifetime measurement is provided in favor of the latter. Polarization effects in light nuclei also influence the determination of spectroscopic quadrupole moments in Coulomb-excitation measurements. The hindrance of polarizability observed in the photo-neutron cross section for single-closed shell nuclei is calculated to have a negligible effect on quadrupole collectivity, within the existing experimental uncertainties.

Keywords: Photo-absorption cross section, $E1$ polarizability, reduced transition probability, spectroscopic quadrupole moment

Virtual excitations are responsible for the polarization of atoms and molecules and give rise to the well-known van der Waals forces between two neutral atoms or molecules, which are far enough apart for the overlap between the wave functions to be neglected [1]. In nuclei, electric-dipole virtual excitations via high-lying states in the giant dipole resonance, GDR [2], can also polarize the ground and excited states of nuclei [3, 5, 4]. This polarization phenomenon is the so-called $E1$ polarizability and is directly related to the static nuclear polarizability, α .

The ability for a nucleus to be polarized is driven by the dynamics of the GDR, i.e., the inter-penetrating motion of proton and neutron fluids out of phase [6]. This motion results in the nuclear symmetry energy, $a_{sym}(A)(\rho_n - \rho_p)^2/\rho$, acting as a restoring force [6, 7]. The nuclear symmetry energy parameter, $a_{sym}(A)$, is key to understanding the elusive equation of state of neutron-rich matter, which impacts three-nucleon forces [8], neutron skins [9, 10], neutron stars and supernova cores [11, 12, 13, 14]. The hydrodynamic model connects α and $a_{sym}(A)$ by [7, 15, 16],

$$\alpha = \frac{e^2 R^2 A}{40 a_{sym}(A)} \text{fm}^3. \quad (1)$$

In nuclear reactions, the induction of an electric dipole moment \mathbf{p} in the nucleus can be generated by the time-dependent electric field \mathbf{E} of the partner. The nuclear polarizability $\alpha = \frac{\mathbf{p}}{\mathbf{E}}$

can also be determined using second-order perturbation theory,

$$\alpha = 2e^2 \sum_n \frac{\langle i \| \hat{E}1 \| n \rangle \langle n \| \hat{E}1 \| i \rangle}{E_\gamma} = \frac{\hbar c}{2\pi^2} \sigma_{-2}, \quad (2)$$

where σ_{-2} is the (-2) moment of the total electric-dipole photo-absorption cross section [4, 17]. This sum rule indicates that large $E1$ matrix elements via virtual excitations of the GDR [18] may polarize the shape of the ground state $|i\rangle$.

In Coulomb-excitation studies, two-step processes of the type $|i\rangle \rightarrow |n\rangle \rightarrow |f\rangle$ (e.g., $0_1^+ \rightarrow 1_{GDR}^- \rightarrow 2_1^+$) can affect the extracted reduced transition probability, i.e., the $B(E2)$ values, and the sign and magnitude of the spectroscopic quadrupole moment, Q_s , of the final excited state $|f\rangle$ [19]. A final state with $J^\pi = 2^+$ is assumed hereafter for excited states. Both the $E1$ polarizability and the reorientation effect, RE, are second-order effects in Coulomb-excitation theory [3, 20, 21, 5]. The RE generates a time-dependent hyperfine splitting of nuclear levels [21], which can be used to determine the nuclear charge distribution in the laboratory frame [20, 21], i.e., Q_s , for states with angular momentum $J \neq 0, \frac{1}{2}$. The angular distribution of the de-excited γ -rays as a function of scattering angle may be enhanced ($Q_s(2_1^+) > 0$) or inhibited ($Q_s(2_1^+) < 0$), hence providing a spectroscopic probe for a measurement of Q_s .

The polarization potential V_{pol} generated by the $E1$ polarizability is proportional to α , and reduces the effective quadrupole interaction $V_{eff}(t)$ in the following manner [19],

$$\begin{aligned} V_{eff}(t) &= V_0(t) (1 - V_{pol}(t)) \\ &= V_0(t) \left(1 - z \frac{a}{r(t)}\right). \end{aligned} \quad (3)$$

Email address: jnorce@uwc.ac.za (J.N. Orce)

URL: <http://www.pa.uky.edu/~jnorce> (J.N. Orce)

For the case of projectile excitation,¹ z is given by Alder and Winther (appendix J) [5],

$$z = \frac{10Z_t\alpha}{3Z_p R^2 a} \approx 0.005\kappa \frac{E_p A_p}{Z_p^2(1 + A_p/A_t)}, \quad (4)$$

with E_p the kinetic energy (in MeV) in the laboratory frame, a the half-distance of closest approach in a head-on collision, $r(t)$ the magnitude of the projectile-target position vector, and α is given by combining² $\alpha = \frac{\hbar c}{4\pi^2}\sigma_{-2}$ [5] and Levinger's empirical formula [15],

$$\sigma_{-2} = 3.5\kappa \times 10^{-4} A^{5/3} \text{ fm}^2/\text{MeV}, \quad (5)$$

where a constant value of $a_{sym} = 23$ MeV is assumed, and the polarizability parameter κ is the ratio of the observed GDR effect for ground states (circles in Fig. 1) to that predicted by the hydrodynamic model [7, 15]. A value of $\kappa = 1$ is broadly accepted since 1957 for $A \geq 20$ nuclei [15]. The general assumption in Coulomb-excitation codes [23, 24] is that the $E1$ polarizability effect for excited states remains the same as the one determined by Levinger for ground states [15]. Equation 5 (for $\kappa = 1$) is plotted (dotted line) in Fig. 1.

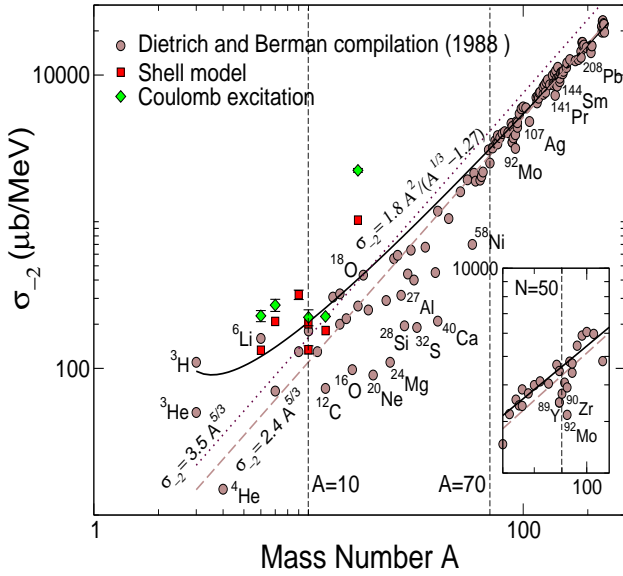


Figure 1: (Color online) The σ_{-2} data vs A on a log-log scale from the 1988 photo-neutron cross-section evaluation (circles) [25], shell model (squares) [26, 27, 28] and Coulomb-excitation (diamonds) [19, 29, 30, 31, 32] studies. For comparison, Eqs. 5 (dotted line), 7 (dashed line) and 11 (solid line) are also plotted. Shell effects are noticeable for the $N = 50$ (inset), $N = 82$ and $N = 126$ isotones.

The factor of 0.005 in front of Eq. 4, the so-called $E1$ polarization parameter, is the default value (for $\kappa = 1$) used in modern Coulomb-excitation codes such as GOSIA [23] and Winther–de Boer [24]. Curiously, Häusser [21] provides an

¹ Similarly, for the case of target excitation, $z \approx 0.005\kappa \frac{E_p A_t}{Z_t^2(1 + A_p/A_t)}$.

² Equation 2 is in better agreement with recent measurements of $\alpha(^{208}\text{Pb}) = 18.9(13) \text{ fm}^3$ using polarized protons [22]. From the empirical value of $\sigma_{-2} = 1.59 \text{ fm}^2/\text{MeV}$ [25] and Eq. 2, $\alpha(^{208}\text{Pb}) = 15.9 \text{ fm}^3$.

equality to Eq. 4 with the actual factor of 0.0056 given by Nakai and Winther's private communication [29, 33], but invoking the right-hand side of Eq. 2. Instead, the factor of 0.005 in Eq. 4 was deduced by Alder and Winther using $\alpha = \frac{\hbar c}{4\pi^2}\sigma_{-2}$ from Ref. [4]. Nevertheless, Eqs. (1.6), (1.7), (1.8), (1.9) and (1.24) in Levinger's monograph [4] yield Eq. 2, in agreement with Migdal [7] and Levinger himself [15]. With the correct use of Eq. 2 [1, 34, 15, 4, 16, 21], the resulting polarization potential is two times larger,

$$z = 0.0112 \kappa \frac{E_p A_p}{Z_p^2(1 + A_p/A_t)}. \quad (6)$$

This enhancement results in a substantial reduction of the effective quadrupole interaction. With the polarization potential in Eq. 6, calculations with the semi-classical coupled-channel Coulomb excitation code GOSIA [23] generally yield (for $\kappa = 1$) an increase of approximately 6% with respect to previously extracted $B(E2)$ values.

This long-standing misunderstanding is fortunately mitigated by a new empirical formula for σ_{-2} [16] determined from the 1988 photo-neutron cross-section evaluation using monoenergetic photons [25],

$$\sigma_{-2} = 2.4\kappa A^{5/3} \mu\text{b}/\text{MeV}. \quad (7)$$

This equation is plotted (dashed line) in Fig. 1. The overall modification of the polarization potential is, therefore,

$$z = 0.0077 \kappa \frac{E_p A_p}{Z_p^2(1 + A_p/A_t)}, \quad (8)$$

which gives an overall increase of 54% with respect to the polarization potential in Eq. 4, and an increase of approximately 3% (for $\kappa = 1$) in previously extracted $B(E2)$ values.

A broader description of the polarization potential naturally arises from the inclusion of $a_{sym}(A)$ in Eq. 1. The mass dependency of $a_{sym}(A)$ has recently been determined by Tian and collaborators [35] from a global fit to the binding energies of isobaric nuclei with $A \geq 10$, extracted from the 2012 atomic mass evaluation [36],

$$a_{sym}(A) = 28.32 \left(1 - 1.27A^{-1/3}\right), \quad (9)$$

where $S_v \approx 28.32$ MeV is the bulk symmetry energy coefficient and $\frac{S_s}{S_v} \approx 1.27$ the surface-to-volume ratio [35]. Equation 9 includes Coulomb energy and shell corrections and, more importantly, opens up the exciting prospect of generic equations for α and σ_{-2} ,

$$\alpha(A) = \frac{1.83 \times 10^{-3} A^2}{A^{1/3} - 1.27} \text{ fm}^3, \quad (10)$$

$$\sigma_{-2}(A) = \frac{1.83 A^2}{A^{1/3} - 1.27} \mu\text{b}/\text{MeV}, \quad (11)$$

which may not require introducing the empirical parameter κ [16]. Equation 11 is plotted in Fig. 1 (solid line) for $A \geq 3$ nuclides, and provides an explanation for the enhancement of

Nucleus	$E_x(\text{MeV})$	J^π	$\sigma_{-2} = 3.5\kappa A^{5/3} \mu\text{b/MeV}$				$\sigma_{-2} = 2.4\kappa A^{5/3} \mu\text{b/MeV}$	
			κ_{SM}	Ref.	κ_{Coulx}	Ref.	κ_{SM}	κ_{Coulx}
${}^6\text{Li}$	2.186	3_1^+	1.9	[26]	3.3(7)	[30]	2.8	4.8(10)
${}^7\text{Li}$	0.478	$1/2_1^-$	2.3	[26]	3.0(7)	[19, 32, 29, 39, 37]	3.4	4.4(10)
${}^9\text{Be}$	0	$3/2_1^-$	2.3(4)	[28]			3.4(6)	
${}^{10}\text{B}$	0.718	1_1^+	1.2	[26]	1.4(4)*	[31]	1.8	2.0(6)*
${}^{10}\text{Be}$	3.368	2_1^+	0.8(2)	[28]			1.2(3)	
${}^{12}\text{C}$	4.439	2_1^+	0.8	[26]	1.0*	[40]	1.2	1.5*
${}^{17}\text{O}$	0.871	$1/2_1^+$	2.6	[27]	5.7(4)	[41]	3.8	8.3(6)

Table 1: Polarizability parameters κ determined from Coulomb-excitation measurements (Coulx) [30, 19, 31, 32, 29] and shell-model calculations [26, 27, 28] using the empirical formulas of Levinger [Eq. 5] and Orce [Eq. 7]. An asterisk indicates that crude estimations were made to determine κ [31, 40].

σ_{-2} observed in light nuclei. However, Eq. 11 becomes negative at $A = 2$. The fact that the GDR has been observed for all nuclei except for the deuteron may support Eq. 11 for $A \geq 3$. The predicted curve nicely merges with the data for $A \gtrsim 70$, in agreement with the dominant photo-neutron cross sections in heavy nuclei [16].

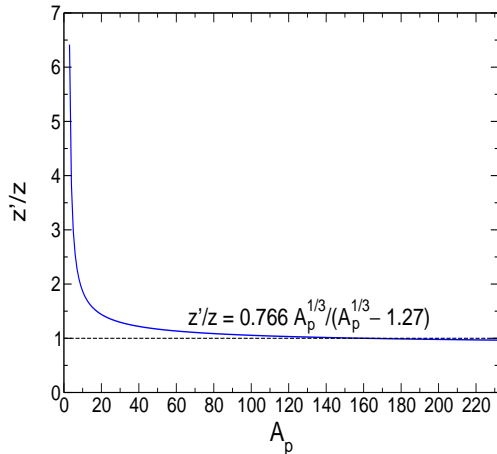


Figure 2: (Color online) Plot of z'/z (as given in Eqs. 8 and 12) vs A for $\kappa = 1$.

Finally, a κ -free polarization potential z' can be obtained inserting Eq. 10 on the left-hand side of Eq. 4,

$$z' = 0.0059 \frac{E_p}{Z_p^2(1 + A_p/A_t)} \frac{A_p^{4/3}}{A_p^{1/3} - 1.27}. \quad (12)$$

A plot of z'/z for $\kappa = 1$ as a function of mass number A is shown in Fig. 2 for $A \geq 3$ nuclides. It is evident that the mass dependence of $a_{sym}(A)$ gives rise to a larger polarization potential z' and an additional enhancement of quadrupole collectivity for light nuclei. It is reassuring to find out that both polarization potentials converge as A increases. The hydrodynamic model still remains to be tested for light nuclei.

The polarizability effect of Eq. 8 on matrix elements extracted from Coulomb-excitation measurements may additionally be enhanced or inhibited depending on the κ value. As shown in Fig. 1, deviations from the smooth trend in Eq. 8 are observed for $A = 4n, T_z = 0$ nuclei ($\kappa < 1$), loosely-bound

light nuclei with $A < 20$ ($\kappa > 1$), and single-closed shell nuclei with $N = 50, N = 82$ and $N = 126$ ($\kappa < 1$). The drop of σ_{-2} below $A \lesssim 50$, including ${}^{58}\text{Ni}$, is due to the missing (γ, p) contributions in the Dietrich and Berman evaluation [25]. The enhancement of σ_{-2} for loosely-bound light nuclei is due to the smaller $a_{sym}(A)$ values [16]. The hindrance of polarizability for single-closed shell nuclei (e.g., as shown in the inset of Fig. 1 for the $N = 50$ isotones) is due to the resistance of more tightly-bound spherical nuclei to be polarized.

Polarizability parameters for excited states in light nuclei have been determined in favorable Coulomb-excitation measurements [30, 19, 31, 32, 29], where the validity of the hydrodynamic model [Eq. 5] was assumed [30, 38, 19, 37, 39, 31, 40, 32, 41]. The reason for the scarcity of experimental work is that there are a few good candidates where κ can be extracted independently of Q_s . The Coulomb-excitation data do not follow the smooth trend predicted by Eq. 11, particularly for ${}^{17}\text{O}$. However, these results were generally extracted from particle spectra and modern particle- γ coincidence measurements will be very useful. In addition, shell model calculations [26, 27, 28] have been performed to compute κ , assuming that all the $E1$ strength from the ground state is concentrated at E_{GDR} [26, 27], and with the no-core shell model [28]. The results are shown in Fig. 1 and listed in Table 1, and have been renormalised according to Eq. 7 (last two columns in Table 1). Large κ parameters are generally determined for loosely-bound light nuclei [19, 31, 40, 30, 38]. It is relevant to investigate deviations from $\kappa \neq 1$ using Eqs. 8 and 12 together with the available information on κ obtained from the photo-absorption cross sections, Coulomb-excitation measurements and shell-model calculations.

Light nuclei present large polarizability parameters of $\kappa > 1$, which can enhance quadrupole collectivity. A curious case is the large $\kappa = 8.3(6)$ determined in ${}^{17}\text{O}$ [41]. As suggested by Kuehner and co-workers [41], a slightly larger than $\kappa > 1$ value in ${}^{18}\text{O}$ would explain the long-standing $\approx 12\%$ discrepancy between the smaller $B(E2; 0_1^+ \rightarrow 2_1^+)$ determined from seven Coulomb excitation measurements, $0.00421(9) \text{ e}^2\text{b}^2$ [42], and the larger one extracted from a high-precision lifetime measurement, $0.00476(11) \text{ e}^2\text{b}^2$, determined by Ball and co-workers in 1982 by fitting the Doppler-broadened γ -ray line-shapes [43]. The latter value nicely agrees with a similar lifetime measurement by Hermans and co-workers [44]. A half-

way $B(E2; 0_1^+ \rightarrow 2_1^+) = 0.00448(13) e^2 b^2$ is determined from an inelastic electron scattering measurement by Norum and collaborators in 1982 [45].

Using Eq. 7, a value of $\kappa \approx 1.8$ for the ground state of ^{18}O is determined from $\sigma_{-2} = 547 \mu\text{b}/\text{MeV}$ [46]. This σ_{-2} value was determined from total photonuclear cross sections, which included $\sigma(\gamma, p)$, $\sigma(\gamma, n) + \sigma(\gamma, np)$, and $\sigma(\gamma, 2n)$, and was integrated from threshold to 42 MeV. As shown in Fig. 2, this relatively large κ value is in agreement with the larger $z'/z \approx 1.5$ observed for $A_p = 18$. Using $\kappa = 1.8$ for the 2_1^+ state in ^{18}O in Eq. 8, a GOSIA calculation of ^{18}O beams at a safe energy of 90 MeV scattered off a ^{208}Pb target with a $[30^\circ, 60^\circ]$ angular coverage yields an increase of $\approx 10\%$ in the $B(E2; 0_1^+ \rightarrow 2_1^+)$ value relative to the one given by Eq. 4. This relative increase is independent of the $\langle 2_1^+ \parallel \hat{E}2 \parallel 0_1^+ \rangle$ and $\langle 2_1^+ \parallel \hat{E}2 \parallel 2_1^+ \rangle$ matrix elements. As shown in Fig. 1 and Table 1, similar or larger enhancements of $B(E2)$ values can be expected for other light nuclei.

For light nuclei, the enhancement of polarizability will also shift the sign and magnitude of Q_s [19, 16] towards the oblate side. For well-deformed nuclei, the quadrupole interaction dominates and low-lying states are more relevant to the 2_1^+ excitation cross section than the $E1$ polarizability [21, 20]. Because of the A_p/Z_p^2 dependence, a large reduction of the excitation cross section occurs for light nuclei, where the effect of the $E1$ polarizability may exceed the reorientation effect [30, 32, 19, 29]. No photo-absorption cross section information is available for radioactive nuclei. However, the renormalised value of $\kappa = 1.2$ (see Table 1) calculated with the no-core shell model for the 2_1^+ state in ^{10}Be [28] yields a shift of approximately $+0.05$ eb in the $Q_s(2_1^+)$ value [47]. This shift aligns better with the no-core shell model calculations of $Q_s(2_1^+)$ in ^{10}Be [28].

The hindrance of polarizability observed in Fig. 1 for single-closed shell nuclei has not previously been addressed and deserves investigation for prominent cases. The inset of Fig. 1 shows a sharp drop of σ_{-2} values for the $N = 50$ isotones. These shell effects arise from the resistance of single-closed shell nuclei to be polarized and are the result of the more bound spherical density distribution caused by the short-range pairing interaction [48]. Considering $\kappa = 0.7$ for the 2_1^+ state in ^{92}Mo , as given by $\sigma_{-2} = 3160 \mu\text{b}/\text{MeV}$ [25] and Eq. 7, a reduction of 3% for the $B(E2; 2_1^+ \rightarrow 0_1^+)$ value is calculated using the polarization potential in Eq. 8. This reduction is not significant within the existing 6% uncertainty [49]. Because of the 30% reduction in Eq. 8, this result agrees with the $B(E2)$ value extracted using the polarization potential in Eq. 4. These GOSIA calculations assume a ^{92}Mo beam at a safe energy of 480 MeV scattering off a ^{208}Pb target with a $[30^\circ, 60^\circ]$ angular coverage.

Additional shell effects are shown in Fig. 3 (left panel) for the Sn isotopes. A sudden drop of $\sigma_{-2} = 6130 \mu\text{b}/\text{MeV}$ for ^{116}Sn [50] is observed relative to the heavier tin isotopes. Although this small drop ($\kappa = 0.93$ using Eq. 7) may hint a weak subshell gap at $N = 66$, it actually increases by 2% the $B(E2; 2_1^+ \rightarrow 0_1^+)$ value determined using Levinger's formula. GOSIA calculations of ^{116}Sn beams at 580 MeV scattered off a ^{208}Pb target with a $[30^\circ, 60^\circ]$ angular coverage cannot accom-

modate, even using a much smaller κ value, the 20% discrepancy between Coulomb-excitation measurements [42, 51] and the high-precision lifetime measurement by Junglaus and co-workers [52].

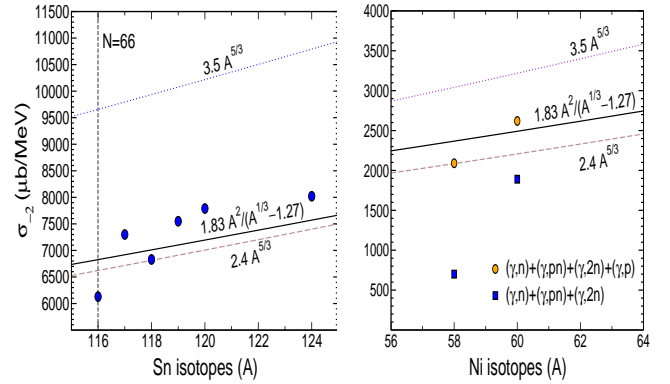


Figure 3: (Color online) Empirical σ_{-2} values available for the Sn (left) and Ni (right) isotopes [50]. For comparison, Eqs. 5, (dotted line), 7 (dashed line) and 11 (solid line) are plotted.

Another peculiar case concerns the smaller $B(E2; 2_1^+ \rightarrow 0_1^+)$ value extracted from a high-precision lifetime measurement by Kenn *et al.* [53], which is several standard deviations from the 2001 evaluation of Raman *et al.* [42]. The right panel of Fig. 1 shows a drop of σ_{-2} in ^{58}Ni . However, once the (γ, p) contribution is added, $\sigma(\gamma, p) \approx 3\sigma(\gamma, n)$ [54], σ_{-2} nicely aligns with Eq. 7 (for $\kappa = 1$). The $B(E2; 2_1^+ \rightarrow 0_1^+)$ value extracted from Coulomb-excitation measurements is only enhanced by approximately 3%, according to Eq. 8, and cannot accommodate the discrepancy between Coulomb-excitation and lifetime measurements. In fact, the extracted $E2$ strengths from lifetime measurements using the inelastic neutron scattering reaction [55] and recent high-precision Coulomb excitation studies by Allmond and collaborators [56] are both in agreement with the 2001 evaluation of Raman *et al.* [42].

In conclusion, new polarization potentials have been determined in this work [Eqs. 8 and 12]. The polarization potential z in Eq. 8 arises from the latest photo-neutron cross section evaluation and a missing factor of two in previous work, and yields an overall increase of 54% with respect to the broadly accepted polarization potential [Eq. 4]. The second one, z' in Eq. 12, opens up the possibility for a κ -free polarization potential based on the mass dependence of $a_{sym}(A)$. A plot of z'/z vs. A shows that the two potentials are essentially the same for heavy nuclei. Moreover, z' explains why light nuclei present an enhanced quadrupole collectivity. Polarization effects in light nuclei affect the determination of $B(E2)$ and Q_s values in Coulomb-excitation studies more than previously assumed. In particular, a value of $\kappa = 1.5$ in ^{18}O deduced from the latest photo-neutron cross section evaluation, and independently by z'/z at $A = 18$, remarkably explains the long-standing discrepancy between the $B(E2; 0_1^+ \rightarrow 2_1^+)$ values determined from seven Coulomb-excitation studies and one high-precision lifetime measurement. A shift of approximately $+0.05$ eb is also determined for $Q_s(2_1^+)$ in ^{10}Be , and results in a better agreement with

no-core shell model calculations. In general, the hindrance of polarization observed in the photo-neutron cross section data has a negligible effect in quadrupole collectivity, within the existing uncertainties.

Finally, it is important to remark the scarce information available concerning the $E1$ polarizability. To date, our knowledge on how nuclei polarize mainly arises from the photo-absorption cross-section data of ground states in stable nuclei. These polarization effects are assumed to behave similarly for excited states populated in the Coulomb excitation of stable and radioactive nuclei. As suggested by Eichler [3] and Häusser [21], modern Coulomb-excitation particle- γ measurements at different bombarding energies and covering large scattering angular ranges present a potential spectroscopic probe to disentangle the $E1$ polarizability and Q_s . These measurements may provide valuable information on deviations from the hydrodynamic model and an alternative probe to constrain $a_{sym}(A)$. Additional experimental and theoretical work are clearly demanded.

The author acknowledges fruitful physics discussions with G. C. Ball, B. A. Brown, S. Triambak, D. H. Wilkinson, J. L. Wood and S. W. Yates. This work was supported by the South African National Research Foundation (NRF) under Grant 93500.

References

- [1] N. F. Mott and I. N. Snedon, *Wave Mechanics and its Applications* (Clarendon Press, Oxford, 1948), Sec. 32.
- [2] K. A. Snover, *Ann. Rev. Nucl. Part. Sci.* **36** (1986) 545.
- [3] J. Eichler, *Phys. Rev.* **133** (1964) B1162.
- [4] J. S. Levinger, *Nuclear Photo-Disintegration* (Oxford University Press, Oxford, 1960).
- [5] K. Alder and A. Winther, *Electromagnetic Excitation* (North-Holland, Amsterdam, 1975).
- [6] A. B. Migdal, *J. Phys. USSR* **8** (1944) 331.
- [7] A. B. Migdal, *J. Exptl. Theoret. Phys. U.S.S.R.* **15** (1945) 81.
- [8] K. Hebelner and A. Schwenk, *Eur. Phys. J. A* **50** (2014) 11.
- [9] M. Centelles, X. Roca-Maza, X. Viñas, and M. Warda, *Phys. Rev. Lett.* **102** (2009) 122502.
- [10] J. Piekarewicz *et al.*, *Phys. Rev. C* **85** (2012) 041302(R).
- [11] A. W. Steiner, M. Prakash, J. M. Lattimer and P. J. Ellis, *Phys. Rep.* **411** (2005) 325.
- [12] J. M. Lattimer, *Nucl. Phys. A* **928** (2014) 276.
- [13] J. M. Lattimer, and M. Prakash, *Phys. Rep.* **333-334** (2000) 121.
- [14] J. M. Pearson, N. Chamel, A. F. Fantina and S. Goriely, *Eur. Phys. J. A* **50** (2014) 43.
- [15] J. S. Levinger, *Phys. Rev.* **107** (1957) 554.
- [16] J. N. Orce, *Phys. Rev. C* **91** (2015) 064602.
- [17] A. B. Migdal, A. A. Lushnikov and D. F. Zaretsky, *Nucl. Phys. A* **66** (1965) 193.
- [18] J. J. Gaardhøje, *Annu. Rev. Nucl. Part. Sci.* **42** (1992) 483-536.
- [19] O. Häusser *et al.*, *Nucl. Phys. A* **212** (1973) 613.
- [20] J. de Boer and J. Eichler, *Adv. Nucl. Phys.* **1** (1968) 1.
- [21] O. Häusser, *Nuclear Spectroscopy and Reactions C*, edited by J. Cerny (Academic, New York, 1974).
- [22] A. Tamii *et al.*, *Phys. Rev. Lett.* **107** (2011) 062502.
- [23] T. Czosnyka, D. Cline, and C. Y. Wu, *Bull. Am. Phys. Soc.* **28** (1983) 745.
- [24] T. E. Drake, Winther-de Boer Coulomb-excitation code (unpublished).
- [25] S. S. Dietrich and B. L. Berman, *Atom. Data Nucl. Data Tables* **38** (1988) 199-338.
- [26] F. C. Barker, *Aust. J. Phys.* **35** (1982) 291.
- [27] F. C. Barker, *Aust. J. Phys.* **35** (1982) 301.
- [28] J. N. Orce *et al.*, *Phys. Rev. C* **86** (2012) 041303(R).
- [29] O. Häusser *et al.*, *Phys. Lett. B* **38** (1972) 75.
- [30] D. L. Disdier *et al.*, *Phys. Rev. Lett.* **27** (1971) 1391.
- [31] W. J. Vermeer *et al.*, *Aust. J. Phys.* **35** (1982) 283.
- [32] A. Bamberger, G. Jansen, B. Povh, D. Schwalm and U. Smilansky, *Nucl. Phys. A* **194** (1972) 193.
- [33] A. Winther, in *Proc. Int. Symp. Nucl. Phys. Tandems*, Heidelberg; private communication (1966).
- [34] E. Merzbacher, *Quantum Mechanics* (Wiley, New York, 1961), p. 446.
- [35] J. Tian, H. Cui, K. Zheng, and N. Wang, *Phys. Rev. C* **90** (2014) 024313.
- [36] M. Wang, G. Audi, A. H. Wapstra, F. G. Kondev, *Chin. Phys. C* **36** (2012) 1603.
- [37] W. J. Vermeer *et al.*, *Aust. J. Phys.* **37** (1984) 273.
- [38] E. B. Bazhanov *et al.*, *Nucl. Phys.* **68** (1965) 191.
- [39] U. Smilansky, B. Povh and K. Traxel, *Phys. Lett. B* **38** (1972) 293.
- [40] W. J. Vermeer *et al.*, *Phys. Lett. B* **122** (1983) 23.
- [41] J. A. Kuehner *et al.*, *Phys. Lett. B* **115** (1982) 437.
- [42] S. Raman, Jr. C. W. Nestor and P. Tikkanen, *At. Data Nucl. Data Tables* **78** (2001) 1.
- [43] G. C. Ball, T. K. Alexander, W. G. Davies, J. S. Foster and I. V. Mitchell, *Nucl. Phys. A* **377** (1982) 268.
- [44] J. A. J. Hermans *et al.*, *Nucl. Phys. A* **284** (1977) 307.
- [45] B. E. Norum *et al.*, *Phys. Rev. C* **25** (1982) 1778.
- [46] J. G. Woodworth *et al.*, *Phys. Rev. C* **19** (1979) 1667.
- [47] J. N. Orce *et al.*, in preparation (2016).
- [48] D. J. Rowe and J. L. Wood, *Fundamentals of Nuclear Models, World Scientific* (2010), p. 410.
- [49] <http://www.nndc.bnl.gov>. (NNDC database).
- [50] S. C. Fultz *et al.*, *Phys. Rev.* **186** (1969) 1255.
- [51] J. M. Allmond *et al.*, accepted for publication in *Phys. Rev. C* (2015).
- [52] A. Jungclaus *et al.* *Phys. Lett. B* **695** (2011) 110.
- [53] O. Kenn *et al.*, *Phys. Rev. C* **63** (2000) 021302(R).
- [54] S. C. Fultz *et al.*, *Phys. Rev. C* **10** (1974) 608.
- [55] J. N. Orce *et al.*, *Phys. Rev. C* **77** (2008) 064301.
- [56] J. M. Allmond *et al.*, *Phys. Rev. C* **90** (2014) 034309.